

Determination of cathode current efficiency for electrodeposition of ferromagnetic cobalt nanowire arrays in nanochannels with extremely large aspect ratio

Ryusei Saeki^{a,*}, Takeshi Ohgai^b

^a Graduate School of Engineering, Nagasaki University, Bunkyo-machi 1-14, Nagasaki 852-8521, Japan

^b Faculty of Engineering, Nagasaki University, Bunkyo-machi 1-14, Nagasaki 852-8521, Japan

ABSTRACT

Cathode current efficiency for the electrodeposition of cobalt from an acidic aqueous solution, which took place in anodized aluminum oxide (AAO) nanochannels with an average diameter of ca. 25 nm, was determined by Faraday's first law of electrolysis. The electrodeposited metallic cobalt crystals were grown as an array of nanowires embedded in the nanochannels. The amount of charge consumed for the electrochemical reduction in the nanochannels was estimated considering the time dependence of the cathode current during the electrodeposition of the cobalt nanowires. Meanwhile, the volume of electrodeposition on the cobalt nanowires was determined from the saturated magnetic moment of the nanowires, which was obtained from the magnetization curves. The cathode current efficiency for the electrodeposition of the cobalt nanowire arrays remained at a high level (over 75%) in the cathode potential ranging from -0.70 V to -0.85 V vs. Ag/AgCl. At the cathode potential of -0.80 V, the cathode current efficiency reached 97%. The texture coefficient $TC_{(002)}$ of the cobalt nanowire arrays increased as the cathodic overpotential for the electrodeposition of cobalt decreased. Due to the extremely large aspect ratio (more than 1000), the cobalt nanowire arrays were spontaneously magnetized in the direction parallel to the long axis of the nanowires. With increasing $TC_{(002)}$, the coercivity and squareness of the cobalt nanowire arrays also increased up to ca. 1.6 kOe and 0.8, respectively, at room temperature.

Introduction

Metallic cobalt crystals with hexagonal close-packed crystal structure (hcp-Co) have an easy magnetization direction in the c -axis, which is normal to the (0 0 2) plane. Therefore, hcp-Co thin films, in which the c -axis is oriented in normal to the film plane, can be applied to a perpendicular magnetic recording medium for improving the data storage capacity in hard disk drives [1]. Such thin magnetic films can be synthesized with an extremely small growth rate (less than 1 nm s^{-1}) under ultra-high vacuum through several processes, such as sputter deposition and molecular beam epitaxy. Furthermore, some researchers have developed a method for synthesizing a cobalt (alloy) thin film with a large growth rate through electrochemical deposition [2,3]. However, only a few reports on the development of a thin magnetic film with perfect perpendicular magnetization performance are available because controlling the crystal orientation and crystal grain shape is difficult.

Recently, large shape anisotropy has been discovered to occur when ferromagnetic metals, such as cobalt, iron, and nickel (or their alloys), are made into a nanowire shape [4–6]. Such ferromagnetic metal nanowires have attracted much attention as novel magnetic materials. In the case of a cylindrical ferromagnetic metal, which has a high aspect ratio (length/diameter), the demagnetizing factor along the direction of

the long axis is very small [7,8]. Hence, the demagnetizing field intensity decreases when an external magnetic field is applied in the direction of the long axis of the cobalt nanowires. In addition, the magnetic properties of nanowires can be improved by adjusting the crystal orientation. Montazer et al. reported that the crystallinity of electrodeposited Co crystals was improved by using pulse electrodeposition [9]. They synthesized nanowires with c -axis orientation in the long-axis direction, whose performance had coercivity greater than 4 kOe [10]. One of the simplest processes for synthesizing a ferromagnetic nanowire array is through template synthesis using electrodeposition of the ferromagnetic metal into cylindrical nanochannels. In previous research works, commercially available polymer membranes [11,12] served as a nanochannel template. However, in many cases, the pore size distribution of a polymer membrane was non-uniform, and the aspect ratio (pore length/pore diameter) was not so large (less than 100). Thus, the realization of a single-domain structure using a commercially available polymer membrane will be very difficult. The structure of an anodized aluminum oxide (AAO) template [13,14] depends on fabrication parameters, such as cell voltage, solution temperature, solution concentration, and reaction time. In other words, a template synthesis technique utilizing an AAO template enables the reduction of the diameter of the cobalt nanowires to realize a single-domain structure.

* Corresponding author.

E-mail addresses: bb52318101@ms.nagasaki-u.ac.jp (R. Saeki), ohgai@nagasaki-u.ac.jp (T. Ohgai).

<https://doi.org/10.1016/j.rinp.2019.102658>

Received 16 July 2019; Received in revised form 10 September 2019; Accepted 11 September 2019

Available online 16 September 2019

2211-3797/© 2019 The Authors. Published by Elsevier B.V. This is an open access article under the CC BY license (<http://creativecommons.org/licenses/by/4.0/>).

Some researchers have reported the fabrication of cobalt nanowire arrays using several techniques involving electrodeposition into AAO nanochannels [15–21]. Most of the reports have focused on the structure and magnetic properties of cobalt nanowire arrays. In a cathodic electrodeposition process from an aqueous solution, the hydrogen ion (H^+) reduction process should be considered in addition to the metal ion reduction process. Therefore, the cathode current efficiency for the electrodeposition of cobalt, which can be determined by Faraday's first law of electrolysis, will affect the morphology and magnetic performance. In particular, the crystal growth process of metals electrodeposited from an aqueous solution is significantly dominated by the cathode current efficiency. Some studies reported the cathode current efficiency for the electrodeposition of two-dimensional thin films or three-dimensional bulk metals [22–24]. Many researches have focused on the magnetic and structural properties of nanowires. However, only a few reports on the current efficiency during electrodeposition into pores are available [25,26]. Arefpour et al. reported that a current efficiency of 91% was achieved in Ni nanowires with a length of 16 μm [25].

Some researchers have also reported the current efficiency for metal electrodeposition in the pores of AAO templates [25,26]. However, the original point of our research is that the amount of charge consumed for the electrochemical reduction was estimated from the time-dependence of the current monitored during potentiostatic electrodeposition. Moreover, the volume of cobalt filling the AAO nanochannels was estimated based on the saturated magnetic moment of the Co nanowire arrays to determine the amount of charge consumed in the reduction of the Co^{2+} ions. Furthermore, the effect of the cathode potential on the cathode current efficiency, growth rate, crystal structure, and magnetic properties of the electrodeposited Co nanowires were investigated.

Methods

First, a cross section of an aluminum rod (purity: 99%) was mechanically and electrochemically polished to obtain a smooth surface. Then, this smooth surface was anodized in 0.3 M sulfuric acid (2 °C to 4 °C) by applying a constant cell voltage of 20 V. An aluminum oxide layer with nanochannel (cylindrical pore) structure was formed on the cross section of the aluminum rod. Subsequently, the barrier layer (the boundary between the metallic aluminum and the aluminum oxide layer) was dissolved through electrochemical etching. Ethanol (99.5 wt %) and perchloric acid (60 wt%) were mixed at a volume ratio of 1:1 to make an electrolytic solution for the electrochemical etching. A gold wire was used as the cathode, and a constant voltage of 35 V was applied to the electrolytic cell for 30 s. After that, the aluminum rod was lightly shaken in a super-pure water to separate the aluminum rod from the aluminum oxide layer. The obtained aluminum oxide film (AAO template) had a nanochannel structure. The pore diameter and average film thickness of the AAO templates were ca. 25 nm and ca. 42 μm , respectively.

Next, a thin gold layer was formed on one side of the AAO template via sputtering, and the AAO template was pasted to a copper chip using a conductive silver paste. The solvents of the silver paste included toluene and ethyl methyl ketone. Then, the copper chip pasted to the AAO template was fixed to a copper plate using polyimide tape to prepare the cathode for the electrodeposition of cobalt. In addition, a gold wire and an Ag/AgCl electrode were prepared as the anode and reference electrode, respectively. The aqueous solution containing 0.5 M cobalt chloride and 0.4 M boric acid (pH buffer) was synthesized as an electrolytic bath for electrodeposition. The temperature of the electrolytic bath was 20 °C, and its pH value was 3.5. Subsequently, cobalt was electrodeposited potentiostatically into the nanochannels of the AAO templates at the cathode potentials of -0.85 , -0.80 , -0.75 , and -0.70 V vs. Ag/AgCl using a Potentiostat/Galvanostat (HA-151, Hokuto Denko Corp., Tokyo, Japan). On the basis of the time dependence of the cathode current, which was measured during the

electrodeposition, we calculated the amount of charge consumed in the total reduction reaction (cobalt deposition and hydrogen evolution) at the cathode (Q_{All}). After the electrodeposition of cobalt, the magnetic properties of the Co nanowire arrays were evaluated using a vibrating-sample magnetometer (TM-VSM1014-CRO, Tamakawa Corp., Sendai, Japan). During the magnetization measurement, an external magnetic field was applied in directions parallel and vertical to the long axis of the Co nanowire. In addition, the volume of cobalt electrodeposited into the nanochannels was estimated from the saturated magnetic moment of the Co nanowire array. In this way, we calculated the amount of charge consumed in the cobalt deposition reaction at the cathode (Q_{Co}). That is, the cathode current efficiency of the cobalt deposition reaction ($\eta_{Co(Nw)}$) was obtained by dividing Q_{Co} by Q_{All} . The cathode current efficiency was calculated using Eq. (1).

$$\eta_{Co(Nw)}(\%) = \frac{Q_{Co}(C)}{Q_{All}(C)} \times 100(\%) \quad (1)$$

Moreover, the crystal orientation of the Co nanowire arrays was evaluated using an X-ray diffractometer (XRD, Miniflex 600-DX, Regaku Corp., Tokyo, Japan). Subsequently, the aluminum oxide part of the Co nanowire arrays was dissolved with 5 M NaOH. Then, the template-free Co nanowire was observed, and its structure was analyzed using a transmission electron microscope (TEM, JEM-2010-HT, JEOL Ltd., Tokyo, Japan).

Results and discussion

Synthesis of cobalt nanowire arrays by potentiostatic electrodeposition

Fig. 1 shows the cathodic polarization curves obtained from an aqueous solution (20 °C, pH 3.5) containing Co^{2+} ions. A copper sheet, a gold wire, and an Ag/AgCl electrode are used as the cathode, anode, and reference electrode, respectively. The cathode potential is scanned in the cathodic direction at a scan rate of 50 $mV s^{-1}$. As shown in the figure, the cathode current density greatly increases at a cathode potential ranging from -0.44 V to -1.0 V vs. Ag/AgCl. On the contrary, the current density gradually increases at the cathode potential region below -1.0 V vs. Ag/AgCl. When the rate-limiting process is charge transfer, the relationship between the current density and overvoltage is expressed by Butler–Volmer equation. In the high-overvoltage region, the Butler–Volmer equation is simplified as the Tafel equation. The Tafel equation is shown in Eq. (2):

$$\eta = a \pm b \ln |i| \quad (2)$$

Based on this equation, the rate-limiting process is the charge transfer in the potential region, which is nobler than -1.0 V vs. Ag/AgCl. Furthermore, in the potential region below -1.0 V, the rate-

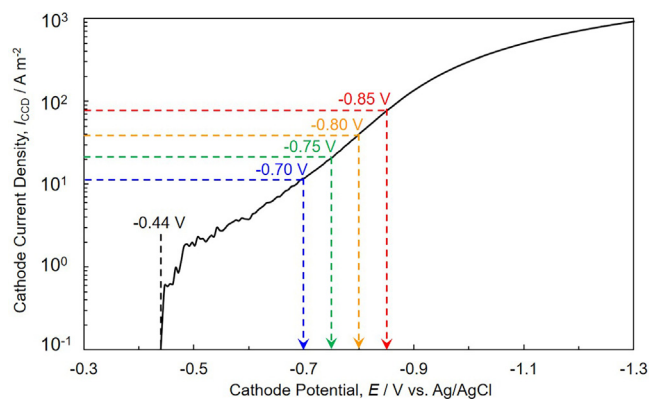


Fig. 1. Cathode polarization curve for Co electrodeposition from an aqueous solution containing $CoCl_2$ and H_3BO_3 . The solution temperature was kept to 20 °C.

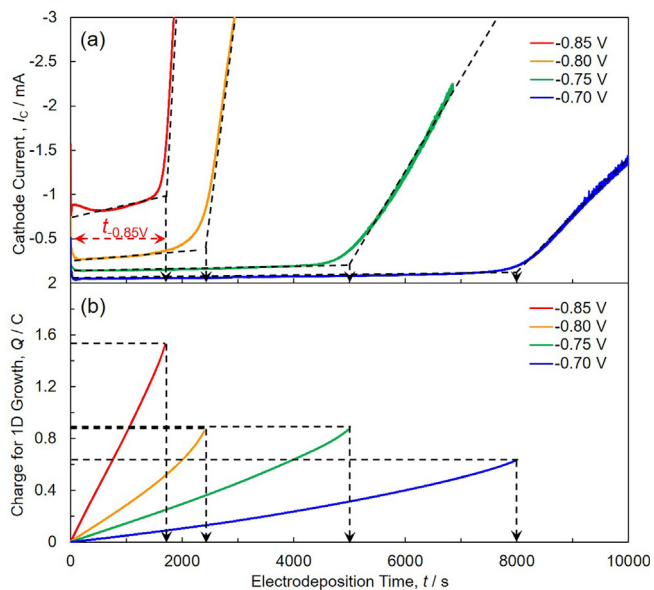


Fig. 2. (a) Time-dependence of cathode current during the electrodeposition of Co nanowires in the nanochannels of anodized aluminum oxide templates. (b) Time-dependence of amount charge for the cathodic reduction.

limiting process is mass transfer. Thus, a cathode potential region nobler than -1.0 V vs. Ag/AgCl is appropriate for the electrodeposition of cobalt. As previously mentioned, in this research, the nanochannel AAO templates were used during the electrodeposition of the cobalt nanowire arrays. The metal ion diffusion coefficient in the nanochannels decreases with an increase in the nanochannel length [27]. Therefore, the cathode potentials -0.85 , -0.80 , -0.75 , and -0.70 V vs. Ag/AgCl are selected here for the electrodeposition of cobalt, as shown in Fig. 1.

Fig. 2(a) shows the time dependence of the cathode current during

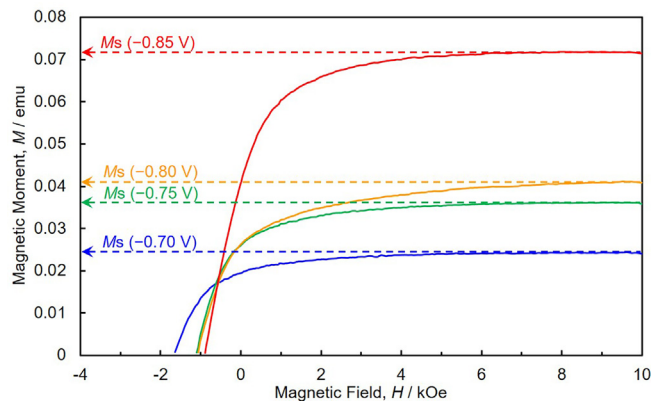


Fig. 4. Magnetization curves for Co nanowire arrays which were electro-deposited at -0.70 V, -0.75 V, -0.80 V and -0.85 V.

the electrodeposition of the Co nanowire arrays. For a while after the start of electrodeposition, the current value remains almost constant. Then, the cathode current begins to dramatically increase from a specific time. The magnitude of the cathode current is in proportion to the area of the cathode. Hence, this dramatic increase in the cathode current is probably caused by the film-like deposition of cobalt on the outside of the nanochannel AAO template. Prior to the magnetic measurement, the film-like cobalt electrodeposited on the surface of nanochannel AAO template is removed by etching with 1 M nitric acid.

Based on the time dependence of the cathode current, the amount of charge consumed in the electrochemical reduction at the cathode, which corresponds to the cobalt deposition and hydrogen evolution, during the one-dimensional (1D) growth of the Co nanowires is shown in Fig. 2(b).

Subsequently, the growth rate of the Co nanowires is calculated by dividing the thickness of the AAO template by the duration of 1D growth of the Co nanowires. Fig. 3(a) (or Fig. 3(b)) shows the

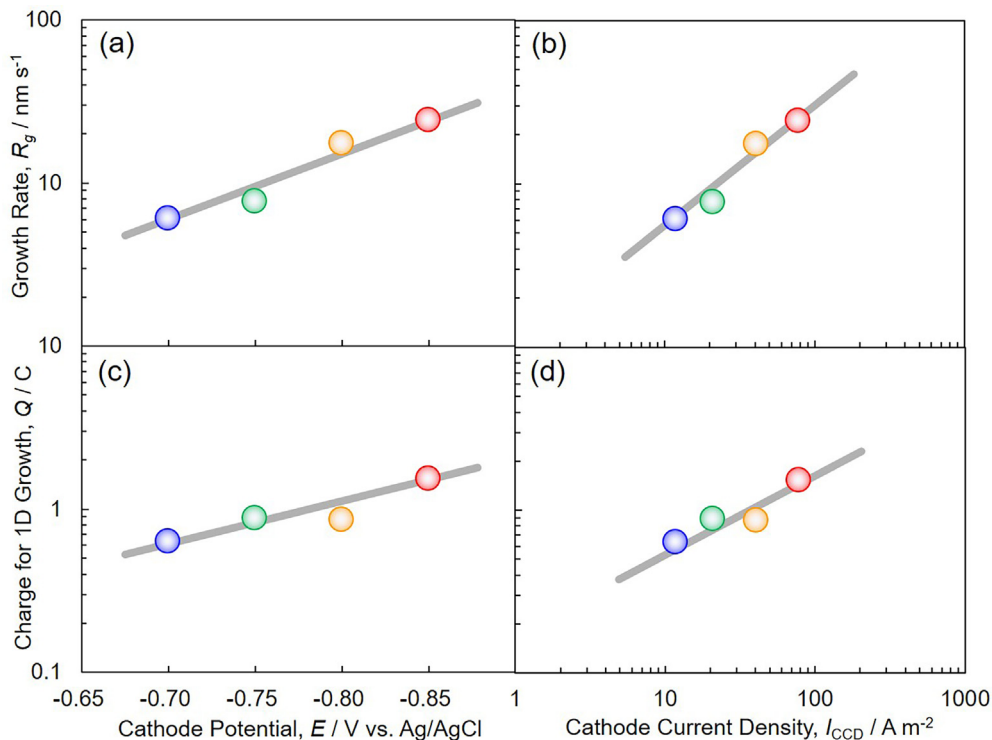


Fig. 3. Effect of cathode potential (a), (c) and cathode current density (b), (d) on the growth rate of electrodeposited Co nanowires and the amount of charge for the cathodic reduction.

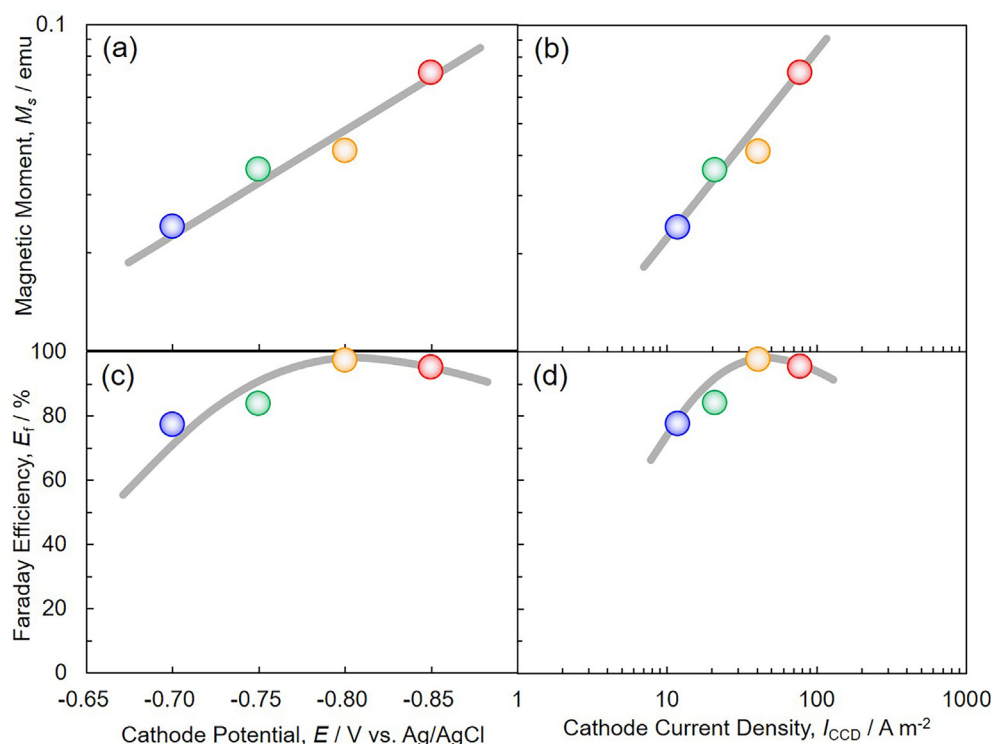


Fig. 5. Effect of cathode potential (a), (c) and cathode current density (b), (d) on the magnetic moment of the electrodeposited Co nanowires and the Faraday efficiency for the cathodic reduction.

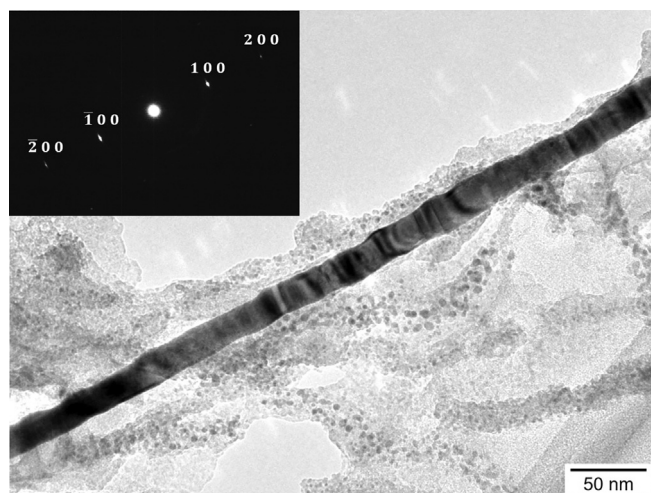


Fig. 6. TEM bright-field image and electron diffraction pattern of Co nanowire that electrodeposited at the cathode potential of -0.80 V vs. Ag/AgCl.

relationship between the growth rate of the Co nanowires and the cathode potential (or the cathode current density). The growth of the Co nanowires tends to increase with the cathodic overpotential or cathode current density. Fig. 3 (c) (or Fig. 3 (d)) shows the relationship between the amount of charge for 1D growth of the Co nanowires and the cathode potential (or the cathode current density). The amount of charge consumed in the electrochemical reduction process at the cathode during the 1D growth of the Co nanowires tends to increase with the cathodic overpotential or the cathode current density.

Calculation of cathode current efficiency of the cobalt deposition process

Fig. 4 shows the magnetization curves of the cobalt nanowire arrays that were electrodeposited at each cathode potential. According to the

magnetization curves, the values of the magnetic moment of the Co nanowire arrays become saturated with the increase of the external magnetic field. The values of the saturated magnetic moment of the Co nanowire arrays increase with the cathodic overpotential (or the cathode current density) by shifting the cathode potential to the less-noble direction (Fig. 4(a) and (b)). On the basis of the values of the saturated magnetic moment of the Co nanowire arrays, we evaluate the volume of the cobalt electrodeposited into the nanochannels of the AAO template. In addition, we evaluate the amount of charge consumed in the cobalt deposition process. Considering the X-ray diffraction patterns of the Co nanowires arrays (Fig. 7), the peaks of hcp-Co are confirmed. Some bubbles are also observed on the surface of the AAO template during the electrodeposition. In this study, the selected cathode potentials are less than the equilibrium potential of hydrogen (-0.197 V vs. Ag/AgCl). Hence, the hydrogen evolution reaction occurs at the cathode during electrodeposition. For these reasons, the amount of charge input is mainly consumed for the reductions of Co^{2+} and H^+ . The cathode current efficiency is calculated using Eq. (1). Fig. 5(c) (or Fig. 5(d)) shows the relationship between the cathode current efficiency of the cobalt deposition reaction and the cathode potential (or the cathode current density). Here, the cathode current efficiency of the cobalt deposition reaction remains at a high level over 75%. Moreover, the cathode current efficiency reaches 97% at the cathode potential of -0.80 V vs. Ag/AgCl. Hence, most of the consumed charge is used for the cobalt deposition reaction. Directly comparing the value of the current efficiency with other reports on electrodeposition of nanowires is difficult because only a few reports have focused on the current efficiency. However, some research works report on the cathode current efficiency for the electrodeposition of cobalt films. Patnaik et al. reported that the current efficiency of 99.6% was achieved by adding tetraethylammonium bromide to the electrolytic bath [23]. Kongstein et al. also reported that the current efficiency for Co electrodeposition using a high-temperature electrolytic bath depended on the concentration of cobalt. In their study, the achieved current efficiency exceeded 80% [24]. On the contrary, in our research, the cathode

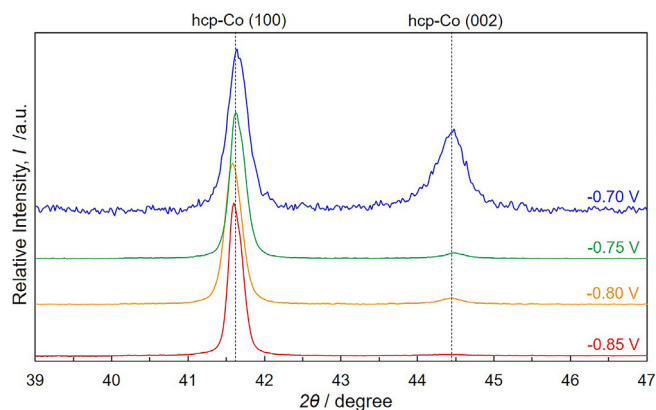


Fig. 7. X-ray diffraction patterns of Co nanowire arrays that were electrodeposited at cathode potential of -0.70 V, -0.75 V, -0.80 V and -0.85 V.

current efficiency during the electrodeposition of the Co nanowire array reached 97%. Therefore, our results are almost consistent with those of other research reports on the current efficiency during cobalt electrodeposition.

We focus on the cathode current efficiency during the potentiostatic electrodeposition into the nanopores of the AAO template. During electrodeposition, the nanowire growth process is monitored by measuring the time dependence of cathode current. A very simple method is proposed for estimating the cathode current efficiency for the reduction of the Co^{2+} ions from the time dependence of the cathode current and the saturated magnetic moment of the Co nanowire array. Furthermore, an optimum cathode potential range is used for achieving the maximum cathode current efficiency.

Analysis of the structure of the cobalt nanowire

Fig. 6 shows a TEM bright-field image and an electron diffraction pattern of the Co nanowire electrodeposited at the cathode potential of -0.80 V vs. Ag/AgCl. A long straight Co nanowire is observed from the bright-field image, and its diameter is estimated at ca. 25 nm. This value corresponds to the pore diameter of the nanochannels of the AAO template. According to the diffraction pattern, the normal direction of the (1 0 0) plane in hcp-Co is parallel to the long axis of the Co nanowire. However, diffraction spots derived from the (0 0 2) plane are not confirmed.

Next, the crystal orientation of the Co nanowire arrays was

evaluated using XRD (Fig. 7). In the XRD patterns, no peak indicating metallic aluminum is confirmed. Therefore, the metallic aluminum part is not included in the AAO template. The peaks at $2\theta = 41.6^\circ$ and $2\theta = 44.5^\circ$ represent the (1 0 0) and (0 0 2) planes of hcp-Co, respectively. Under the present experimental conditions, all samples have (1 0 0) crystal orientation. This finding is consistent with the results of the electron diffraction. In addition, when the cathodic overpotential decreases by shifting the cathode potential to the noble direction, we observe the (0 0 2) crystal orientation. Based on theoretical calculations and experiments, Pangarov et al. reported that the (0 0 2) plane of hcp-Co is the preferred orientation plane when the overpotential was decreased during the electrodeposition of cobalt [28]. Our experimental results are consistent with this trend. Indeed, the preferred orientation plane of the Co nanowires can be controlled by adjusting the cathodic overpotential. Subsequently, based on the X-ray diffraction patterns of the Co nanowire arrays, the texture coefficients $TC_{(hkl)}$ are calculated using the Harris equation [29,30]:

$$TC_{(hkl)} = \frac{I_{hkl}^i / I_{hkl}^0}{1/N \times \sum_{j=1}^N (I_{hkl}^j / I_{hkl}^0)} \quad (3)$$

Eq. (3) describes the analysis of the relative peak intensities dependent on I_{hkl} , i.e., the intensities observed from the (hkl) lattice planes of the sample, and I_{hkl}^0 denotes the intensities of a standard Co powder. N is the number of diffraction planes considered for the determination of $TC_{(hkl)}$. Fig. 8(a) shows the relationship between the texture coefficients $TC_{(hkl)}$ and the cathode potential. $TC_{(002)}$ tends to increase with decreasing cathodic overpotential. Moreover, Fig. 8(b) shows the relationship between the texture coefficients $TC_{(hkl)}$ and the volume of cobalt electrodeposited into the nanochannels of the AAO template. $TC_{(002)}$ increases as the volume of cobalt filling the nanochannels decreases.

Evaluation of the magnetic properties of the cobalt nanowire arrays

Fig. 9 shows the magnetic hysteresis loops of the cobalt nanowire arrays that are electrodeposited at each cathode potential ranging from -0.85 V to -0.70 V vs. Ag/AgCl. The external magnetic field (-10 kOe \sim $+10$ kOe) is applied in directions parallel (continuous line) and vertical (dotted line) to the long axis of the Co nanowire. The shape of the magnetic hysteresis loop depends on the direction of the external applied magnetic field. The coercivity and squareness (the ratio between saturated magnetization and residual magnetization) increase when the external magnetic field is applied in the direction parallel to the long axis of the Co nanowire. When a ferromagnetic metal has a

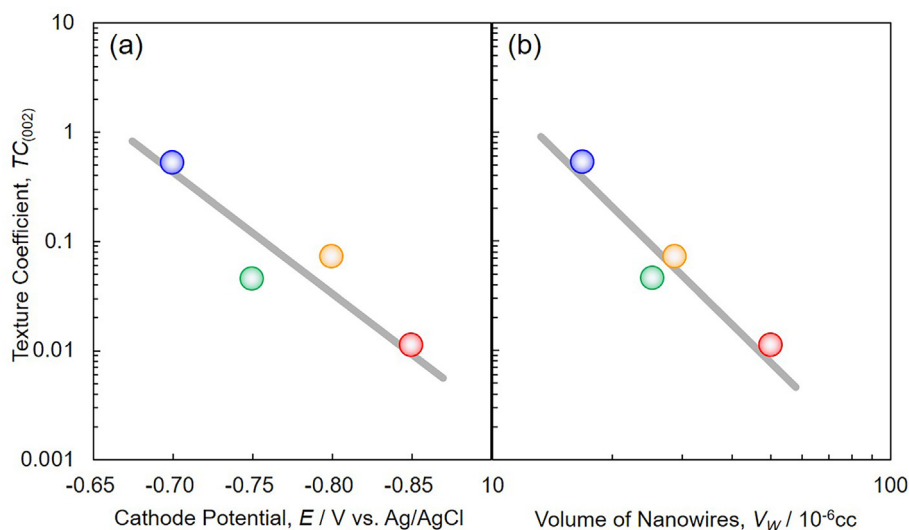


Fig. 8. Effect of cathode potential (a) and volume of nanowires (b) on the texture coefficient TC_{002} of electrodeposited Co nanowire arrays.

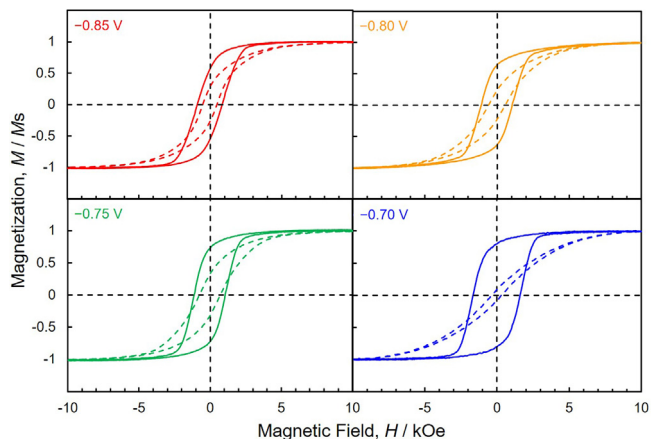


Fig. 9. Magnetic hysteresis loops of Co nanowire arrays that were electrodeposited at -0.85 V, -0.80 V, -0.75 V and -0.70 V in AAO nanochannel films. Magnetic field was applied in parallel (continuous lines) and vertical (dotted lines) to the long axis of Co nanowires.

cylindrical shape, the effect of the demagnetizing field along the direction of the long axis will dramatically decrease. Hence, this magnetic anisotropy seems to be caused by the cylindrical shape of the nanowires, which have a high aspect ratio.

Here, the AAO templates used for electrodeposition at each cathode potential are synthesized by the same method. Hence, the shapes of the nanowires, which are obtained from different samples, are almost the

same. However, the Co nanowire arrays electrodeposited at each cathode potential show different values of coercivity and squareness. Fig. 10 (a) and (d) show the effect of the cathode potential on the coercivity and squareness of the Co nanowire arrays in the magnetic field direction parallel to the long axis of the nanowires. The coercivity and squareness of the Co nanowire arrays increase with decreasing cathodic overpotential. In the case of the Co nanowire arrays, which are electrodeposited at the cathode potential of -0.70 V vs. Ag/AgCl, the coercivity and the squareness increase up to 1.6 kOe and ca. 0.8, respectively, at room temperature. In a similar way, Fig. 10 (b) and (e) show the effect of the volume of cobalt inside the nanochannels on the coercivity and squareness of the Co nanowire arrays. The coercivity and squareness of the Co nanowire arrays increase as the volume of Co filling the nanochannels decreases. Moreover, Fig. 10 (c) and (f) show the effect of the texture coefficients $TC_{(002)}$ on the coercivity and squareness of the Co nanowire arrays. The coercivity and squareness of the Co nanowire arrays increase with $TC_{(002)}$. As shown in Fig. 5, the saturated magnetic moment of the Co nanowire arrays decreases with decreasing cathodic overpotential. The magnetic dipolar interaction between the nanowires decreases with decreasing Co volume and the number of Co nanowires. In addition, as shown in Fig. 8, the texture coefficient $TC_{(002)}$ increases with decreasing cathodic overpotential. The improvement of the hard magnetic properties is caused by a correspondence between the axial direction of the Co nanowire and the c -axis of the hcp-Co crystal. For these reasons, a difference in the magnetic properties exists between the samples.

In this research, the Co nanowire arrays are synthesized using potentiostatic electrodeposition. The samples are not specially treated

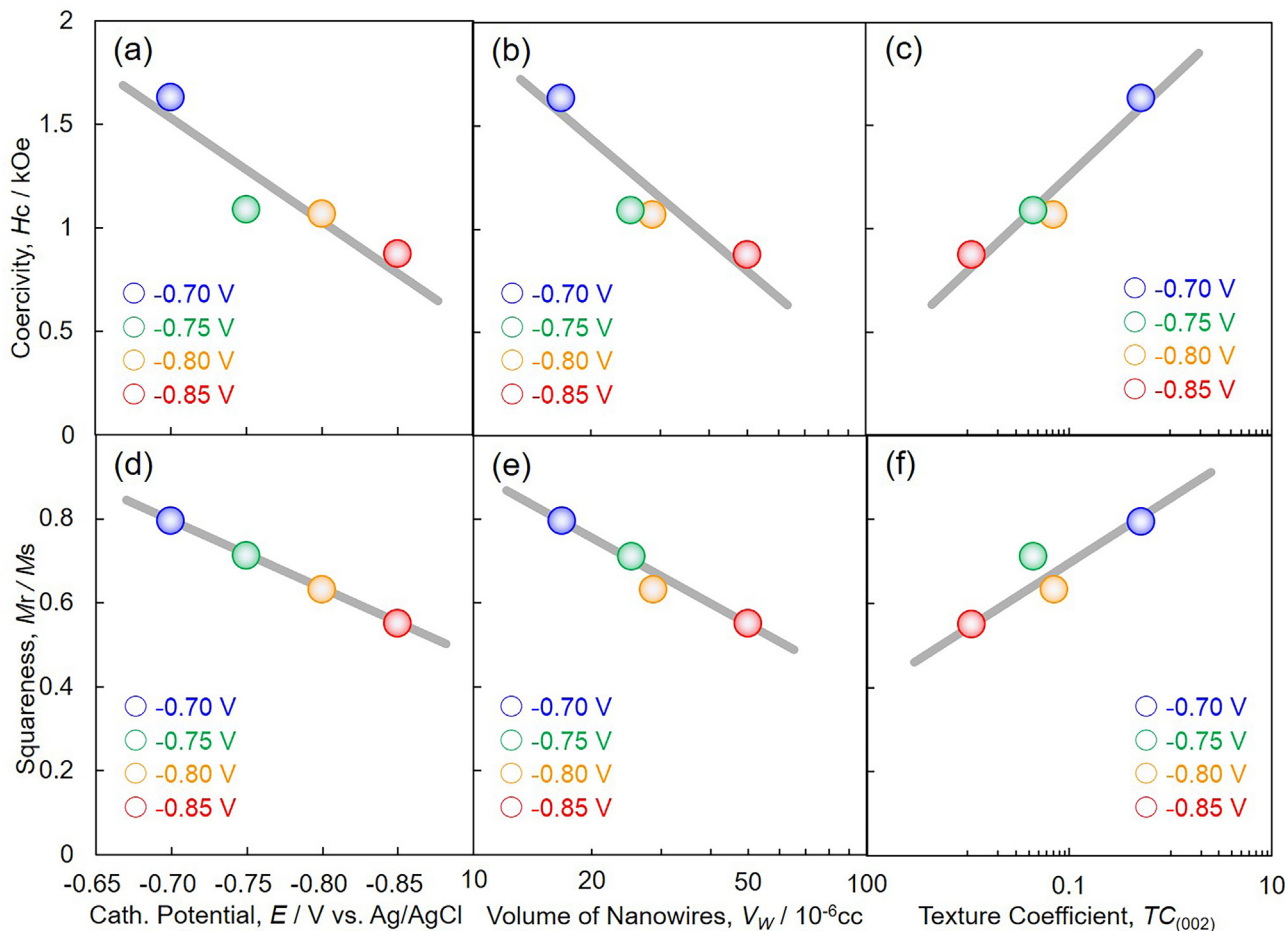


Fig. 10. Effect of cathode potential (a), (d), volume of nanowires (b), (e) and texture coefficient (c), (f) on the coercivity and squareness of electrodeposited Co nanowire arrays.

during or after electrodeposition. Moreover, the temperature and pH of the electrolytic bath are kept constant. However, the electrolysis conditions during electrodeposition have great influence on the crystal structure and magnetic properties of the synthesized Co nanowire arrays. For example, the magnetic properties of Co nanowire arrays are affected by the external magnetic field during electrodeposition and by the electrolyte acidity and annealing process after electrodeposition [5]. In addition, Ramazani et al. improved the coercivity of Co nanowire arrays by pulsed AC electrodeposition [9]. Hence, the optimization of the electrolysis conditions and post-treatment processing lead to further improvement of the magnetic properties of the Co nanowire arrays.

Conclusions

Co nanowire arrays were synthesized by electrochemical reduction of Co^{2+} ions in the nanochannels of AAO templates. With reference to the time dependence of the cathode current during the electrodeposition of the Co nanowires, we calculated the amount of charge (Q_{Al}) consumed in the total reduction reaction (mainly cobalt deposition and hydrogen evolution) at the cathode. The volume of cobalt filling the nanochannels was estimated from the values of the saturated magnetic moment to calculate the amount of charge consumed in the cobalt deposition process (Q_{Co}). The cathode current efficiency in the Co deposition process, which was obtained from the ratio of Q_{Co} to Q_{Al} , showed values greater than 75%. At the cathode potential -0.80 V vs. Ag/AgCl, the cathode current efficiency reached 97%.

The preferential orientation of hcp-Co (002), which corresponded to the *c*-axis in the long axis of the nanowire, was observed when the cathodic overpotential was fixed to a nobler region during the electrodeposition. Hence, the coercivity and squareness of the Co nanowire arrays increased with an increase in $TC_{(002)}$. In the case of the Co nanowire arrays which were electrodeposited at the cathode potential of -0.70 V vs. Ag/AgCl, the coercivity and the squareness were increased and achieved 1.6 kOe and ca. 0.8, respectively, at room temperature.

Author statement

Ryusei Saeki carried out experiments, analyzed data, and wrote the manuscript. Takeshi Ohgai designed the study, supervised the project, and analyzed data. All authors read and approved the final manuscript.

Acknowledgements

The authors thank Japan Science and Technology Agency, Japan (JST: AS262202450K), the Japan Society for the Promotion of Science, Japan (JSPS: 15K06508 and 18H01754) and IKETANI Science and Technology Foundation, Japan (0271040-A) for the financial support.

References

- [1] Marchon B, Pitchford T, Hsia YT, Gangopadhyay S. The head-disk interface roadmap to an areal density of Tbit/in². *Adv Tribol* 2013;2013:521086.
- [2] Munford ML, Seligman L, Sartorelli ML, Voltolini E, Martins LFO, Schwarzacher W, et al. Electrodeposition of magnetic thin films of cobalt on silicon. *J Magn Mater* 2001;226–230:1613–5.
- [3] Borges JG, Prod'homme P, Maroun F, Cortès R, Geshev J, Schmidt JE, Allongue P. Perpendicular anisotropy in electrodeposited Au/Co films. *Phys B* 2006;384:138–40.
- [4] Vien GN, Rioual S, Gloaguen F, Rouvellou B, Lescop B. Study of the magnetization behavior of ferromagnetic nanowire array: existence of growth defects revealed by micromagnetic simulations. *J Magn Mater* 2016;401:378–85.
- [5] Shaterabadi Z, Soltanian S, Koohbor M, Salimi A, Servati P. Modification of microstructure and magnetic properties of electrodeposited Co nanowire arrays: a study of the effect of external magnetic field, electrolyte acidity and annealing process. *Mater Chem Phys* 2015;160:389–97.
- [6] Dong X, Qi M, Tong Y, Ye F. Solvothermal synthesis of single-crystalline hexagonal cobalt nanofibers with high coercivity. *Mater Lett* 2014;128:39–41.
- [7] Prozorov R, Kogan VG. Effective demagnetizing factors of diamagnetic samples of various shapes. *Phys Rev Appl* 2018;10:014030.
- [8] Sato M, Ishii Y. Simple and approximate expressions of demagnetizing factors of uniformly magnetized rectangular rod and cylinder. *J Appl Phys* 1989;66:983–5.
- [9] Ramazani A, Kashi MA, Montazer AH. Fabrication of single crystalline, uniaxial single domain Co nanowire arrays with high coercivity. *J Appl Phys* 2014;115(11):113902.
- [10] Montazer AH, Ramazani A, Kashi MA. Magnetically extracted microstructural development along the length of Co nanowire arrays: the interplay between deposition frequency and magnetic coercivity. *J Appl Phys* 2016;120(11):113902.
- [11] Ohgai T, Mizumoto M, Nomura S, Kagawa A. Single crystalline ferro-magnetic metal nanowires electrodeposited into nanoporous polycarbonate film. *e-J Surf Sci Nanotechnol* 2006;4:1–5.
- [12] Sánchez-Barriga J, Lucas M, Rivero G, Marin P, Hernando A. Magneto-electrolysis of Co nanowire arrays grown in a track-etched polycarbonate membrane. *J Magn Mater* 2007;312:99–106.
- [13] Masuda H, Hasegawa F, Ono S. Self-ordering of cell arrangement of anodic porous alumina formed in sulfuric acid solution. *J Electrochem Soc* 1997;144:L127–30.
- [14] Masuda H, Asoh H, Watanabe M, Nishio K, Nakao M, Tamamura T. Square and triangular nanohole array architectures in anodic alumina. *Adv Mater* 2001;13:189–92.
- [15] Nath K, Sinha J, Banerjee SS. Flipping anisotropy and changing magnetization reversal modes in nanoconfined Cobalt structures. *J Magn Mater* 2019;476:412–6.
- [16] Irshad MI, Mohamed NM, Abdullah MZ, Saheed MSM, Mumtaz A, Yasar M, et al. Influence of the electrodeposition potential on the crystallographic structure and effective magnetic easy axis of cobalt nanowires. *RSC Adv* 2016;6:14266–72.
- [17] Ohgai T, Mizumoto M, Nomura S, Kagawa A. Electrochemical fabrication of metallic nanowires and metal oxide nanopores. *Mater Manuf Processes* 2007;22(4):440–3.
- [18] Barriga-Castro ED, García J, Mendoza-Resendez R, Pridab VM, Luna C. Pseudo-monocrystalline properties of cylindrical nanowires confined grown by electrodeposition in nanoporous alumina templates. *RSC Adv* 2017;7:13817–26.
- [19] Saeki R, Ohgai T. Effect of growth rate on the crystal orientation and magnetization performance of cobalt nanocrystal arrays electrodeposited from aqueous solution. *Nanomaterials* 2018;8(8):566.
- [20] Saeki R, Ohgai T. Determination of activation overpotential during the nucleation of hcp-cobalt nanowires synthesized by potentiostatic electrochemical reduction. *Materials* 2018;11(12):2355.
- [21] Saeki R, Ohgai T. Determination of crystal growth geometry factors and nucleation site densities of electrodeposited ferromagnetic cobalt nanowire arrays. *Crystals* 2019;9(3):142.
- [22] Pradhan N, Singh P, Tripathy BC, Das SC. Electrowinning of cobalt from acidic sulphate solutions—effect of chloride ion. *Miner Eng* 2001;14:775–83.
- [23] Patnaik P, Padhy SK, Tripathy BC, Bhattacharya IN, Paramguru RK. Electrodeposition of cobalt from aqueous sulphate solutions in the presence of tetra ethyl ammonium bromide. *Trans Nonferrous Met Soc China* 2015;25:2047–53.
- [24] Kongstein OE, Haarberg GM, Thonstad J. Current efficiency and kinetics of cobalt electrodeposition in acid chloride solutions. Part II: the influence of chloride and sulphate concentrations. *J Appl Electrochem* 2007;37:675–80.
- [25] Arefpour M, Kashi MA, Ramazani A, Montazer AH. Electrochemical pore filling strategy for controlled growth of magnetic and metallic nanowire arrays with large area uniformity. *Nanotechnology* 2016;27(27):275605.
- [26] Sousa CT, Leitão DC, Proença MP, Apolinário A, Correia JG, Ventura J, et al. Tuning pore filling of anodic alumina templates by accurate control of the bottom barrier layer thickness. *Nanotechnology* 2011;22(31):315602.
- [27] Kaur D, Pandya DK, Chaudhary S. Texture changes in electrodeposited cobalt nanowires with bath temperature. *J Electrochem Soc* 2012;159:D713–6.
- [28] Pangarov NA, Vitkova SD. Preferred orientation of electrodeposited cobalt crystallites. *Electrochim Acta* 1966;11:1733–45.
- [29] Duan J, Liu J, Cornelius TW, Yao H, Mo D, Chen Y, et al. Magnetic and optical properties of cobalt nanowires fabricated in polycarbonate ion-track templates. *Nucl Instr Meth Phys Res B* 2009;267:2567–70.
- [30] Harris GBX. Quantitative measurement of preferred orientation in rolled uranium bars. *Lond, Edinburgh, Dublin Philos Mag J Sci* 1952;43:113–23.